ISSN 1674-1056
http://cpb.iphy.ac.cn
http://iopscience.iop.org/cpb
中国物理 B
Chinese Physics
中国物理 Chinese Physics B

Investigation of the substituent effect on the excited state intramolecular proton transfer of 3-hydroxychromone

Yuzhi Song(宋玉志), Songsong Liu(刘松松), Jiajun Lu(陆佳骏), Hui Zhang(张慧), Changzhe Zhang(张常哲), Jun Du(杜军)
Citation: Chin. Phys. B . 2019, 28(9): 093102 . **doi:** 10.1088/1674-1056/28/093102
Journal homepage: http://cpb.iphy.ac.cn; http://iopscience.iop.org/cpb

What follows is a list of articles you may be interested in

Tensile-strain induced phonon splitting in diamond

Meifang Pu(蒲梅芳), Feng Zhang(张峰), Shan Liu(刘珊), Tetsuo Irifune(入舩徹男), Li Lei(雷力)
Chin. Phys. B . 2019, 28(5): 053102 . **doi:** 10.1088/1674-1056/28/5/053102

Excited state intramolecular proton transfer mechanism of o-hydroxynaphthyl phenanthroimidazole

Shuang Liu(刘爽), Yan-Zhen Ma(马艳珍), Yun-Fan Yang(杨云帆), Song-Song Liu(刘松松), Yong-Qing Li(李永庆), Yu-Zhi Song(宋玉志)
Chin. Phys. B . 2018, 27(2): 023103 . **doi:** 10.1088/1674-1056/27/2/023103

Structural stability of ultra-high temperature refractory material $MoSi_2$ and Mo_5Si_3 under high pressure

Hao Liang(梁浩), Fang Peng(彭放), Cong Fan(樊聪), Qiang Zhang(张强), Jing Liu(刘景), Shi-Xue Guan(管诗雪)
Chin. Phys. B . 2017, 26(5): 053101 . **doi:** 10.1088/1674-1056/26/5/053101

Ab initio path-integral molecular dynamics and the quantum nature of hydrogen bonds

Yexin Feng(冯页新), Ji Chen(陈基), Xin-Zheng Li(李新征), Enge Wang(王恩哥)
Chin. Phys. B . 2016, 25(1): 013104 . **doi:** 10.1088/1674-1056/25/1/013104

Theoretical study of *γ*-aminobutyric acid conformers： Intramolecular interactions and ionization energies

Wang Ke-Dong, Wang Mei-Ting, Meng Ju
Chin. Phys. B . 2014, 23(10): 103101 . **doi:** 10.1088/1674-1056/23/10/103101

The substituent effect on the excited state intramolecular proton transfer of 3-hydroxychromone*

Yuzhi Song(宋玉志)†, Songsong Liu(刘松松), Jiajun Lu(陆佳骏), Hui Zhang(张慧), Changzhe Zhang(张常哲), and Jun Du(杜军)‡

Shandong Province Key Laboratory of Medical Physics and Image Processing Technology, School of Physics and Electronics, Shandong Normal University, Jinan 250358, *China*

(Received 13 June 2019; revised manuscript received 5 July 2019; published online 30 August 2019)

The excited state intramolecular proton transfer of four derivatives (FM, BFM, BFBC, CCM) of 3-hydroxychromone is investigated. The geometries of different substituents are optimized to study the substituent effects on proton transfer. The mechanism of hydrogen bond enhancement is qualitatively elucidated by comparing the infrared spectra, the reduced density gradient, and the frontier molecular orbitals. The calculated electronic spectra are consistent with the experimental results. To quantify the proton transfer, the potential energy curves (PECs) of the four derivatives in S_0 and S_1 states are scanned. It is concluded that the ability of proton transfer follows the order: FM > BFM > BFBC > CCM.

Keywords: excited state intramolecular proton transfer (ESIPT), hydrogen bond, reduced density gradient (RDG), substituents

PACS: 31.15.ae, 31.15.A–, 31.15.es **DOI:** 10.1088/1674-1056/ab3434

1. Introduction

Since the beginning of the last century, the photochemistry has become an integrated science to study the generation of excited states, the structure of excited states, and the accompanying physical properties and chemical behaviors.[1,2] Hydrogen bonds are one of the most common weak interactions and widely found in water, proteins, amino acids, alcohols, etc.[3–7] Therefore, on the basis of continuous exploration of the excited state dynamics, the study of excited state hydrogen bonds is very powerful for the advancement of the natural sciences. The excited state intramolecular proton transfer (ESIPT) reaction was firstly observed and reported by Weller *et al.*,[8] and since then it has attracted great interest due to its wide application in molecular probes and luminescent materials.[9–16] In addition, some relevant chemical and biological processes can be explained through investigating the ESIPT reaction in detail, such as a lot of reactions in biological systems containing DNA-based tautomers and photosynthesis. Han and collaborators have studied comprehensively the photoinduced electron transfer (PET), intramolecular or intermolecular charge transfer (ICT), ESIPT, fluorescence quenching mechanism, and so forth.[17–22] Upon the photo-excitation, the molecule can be excited to an unstable state and proton transfer can occur. The power required for proton transfer is derived from the energy gap between the local and the relaxed excited states.

According to previous reports, Yang *et al.* studied the mechanism of the photo-induced contamination reaction by the ESIPT of cresol derivatives.[23] Dong *et al.* reported the ESIPT reaction of 2,6-dibenzothiazolylphenol with its derivatives and the fluoride-sensing mechanism.[24] Hao *et al.* explored the effect of changing the solvent and heterocyclic ring on the ESIPT reaction of three photosensitive monoformylated benzoxazole derivatives.[25] Designing molecules with different substituents can directly affect the photochemical and photophysical properties of the molecules. For instance, solvatochromic probe can explore the living cells of biological molecules by comparing the change in fluorescence behavior. Therefore, it has been widely used in fluorescence sensing technology, organic light-emitting diodes (OLEDs), and molecular probe design.[26–37] Solvatochromic probe is a very effective way to explore the living cells of biological molecules by comparing the change in fluorescence behavior. Kyriukha *et al.* synthesized a series of benzochromones with a red-shifted absorbance based on 3-hydroxybenzochromones (3HCs) as shown in Fig. 1. Three derivatives BFM, CCM, 2-(6-dimethylaminobenzofuryl)-3-Hydroxybenzochromone (BFBC) are derived from the introduction of a fused benzene ring and substituents with extended π-electron conjugated system at position 2 on the parent FM.[38] It was concluded that BFBC is the most suitable fluorescent microscope dye by comparing the fluorescence changes of four different substituted molecules and the polarity sensitivity changes of the dye environment.

We are then motivated to study the effects of different substituents on ESIPT in detail. All calculations for 3HCs

*Project supported by the National Natural Science Foundation of China (Grant Nos. 11874241, 11847224, and 11804195), the Shandong Province Higher Educational Science and Technology Program, China (Grant No. J15LJ03), the Taishan Scholar Project of Shandong Province, China, China Post-Doctoral Foundation (Grant No. 2018M630796), and the Natural Science Foundation of Shandong Province, China (Grant No. ZR2018BA034).

†Corresponding author. E-mail: yzsong@sdnu.edu.cn

‡Corresponding author. E-mail: dujun@sdnu.edu.cn

© 2019 Chinese Physical Society and IOP Publishing Ltd

derivatives are based on the B3LYP-D3 functional with the 6-311+g(d,p) basis set. The effects of hydrogen bond strength on proton transfer can be derived from the analysis of infrared (IR) vibration spectra, electron spectra, frontier molecular orbitals (FMOs), and reduced density gradient (RDG). Moreover, the reaction paths of ESIPT of 3HCs derivatives (FM, BFM, BFBC, and CCM) are analyzed.

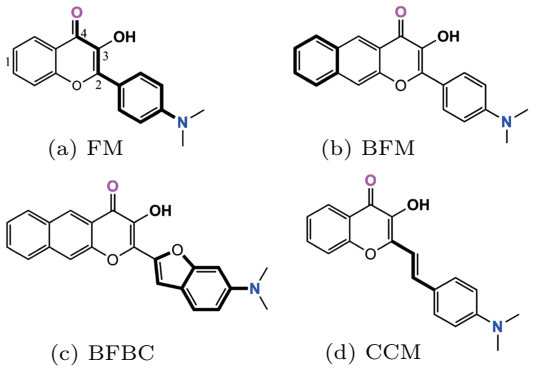


Fig. 1. Molecular structures of 3HCs derivatives: (a) FM, (b) BFM, (c) BFBC, and (d) CCM.

2. Computational details

By employing the Becke's three-parameter hybrid exchange function with the Lee–Yang–Parr gradient-corrected correlation functional (B3LYP-D3) and 6-311+G(d,p) basis set, all the *ab initio* calculations are carried out in the Gaussian 16 program.[39–41] The ground (S_0) state and the first excited (S_1) state of the molecules are optimized using the density functional theory (DFT) and time-dependent density functional theory (TDDFT) methods,[42] respectively. In order to simulate the solvent environment of the experiment, the toluene solvent with a dielectric constant (ε) of 2.37 is used throughout the calculation process with the polarizable continuum model (IEFPCM).[43] In addition, we have calculated the vibration frequencies in order to confirm that the optimized structures are the real minimum. Since the resonance approximation generally overestimates the vibration frequency, the zero point energy correction and Gibbs free energy thermal correction are used to correct the vibration frequency. In order to clearly observe hydrogen bond interactions, the weak interaction regions are represented by the RDG isosurface obtained by using the Multiwfn and VMD programs, where the RDG can be expressed as[44,45]

$$\mathrm{RDG}(r) = \frac{1}{2\left(3\pi^2\right)^{1/3}} \frac{\nabla\rho(r)}{\rho(r)^{4/3}}, \tag{1}$$

$$\Omega(r) = \mathrm{sign}\left(\lambda_2(\gamma)\right)\rho(\gamma). \tag{2}$$

Moreover, the potential energy curves (PECs) of 3HCs derivatives are obtained by flexible scanning.

3. Results and Discussion

3.1. Optimization of geometric structures

In order to facilitate the comparison of the hydrogen bond interaction of the S_0 state and S_1 state of the 3HCs derivatives (FM, BFM, BFBC, and CCM), the B3LYP/6-311+G(d,p) are to be adopted to optimized their geometric structures, which are displayed in Fig. 2. The major bond lengths and bond angles associated with hydrogen bonds are gathered in Table 1. As shown in Table 1, the O_1–H_2 bond lengths in the enol form of FM, BFM, BFBC, and CCM are 0.981 Å, 0.974 Å, 0.973 Å, and 0.978 Å in the S_0 state, respectively. The H_2–O_3 bond lengths are 1.993 Å, 1.963 Å, 2.011 Å, and 2.073 Å. The bond angles (O_1–H_2–O_3) are 119.6°, 120.1°, 118.8°, and 117.3°, respectively. However, when they are in the S_1 state, the O_1–H_2 bond lengths increase to 0.993 Å, 0.991 Å, 0.985 Å, and 0.981 Å. The H_2–O_3 bond lengths are reduced to 1.794 Å, 1.808 Å, 1.873 Å, and 1.950 Å, while the bond angles are increased to 126.1°, 125.1°, 123.5°, and 121.2°. Such changes show that the hydrogen bond interactions of 3HCs derivatives are strengthened in the S_1 state. However, when the molecules return from the S_1 state to the S_0 state, the O_1–H_2 bond lengths of keto form decrease from 1.984 Å, 1.942 Å, 1.937 Å, and 2.030 Å to 1.822 Å, 1.817 Å, 1.818 Å, and 1.889 Å, which indicates that the hydrogen bonds in the keto forms of the 3HCs derivatives are stronger in the S_0 state than in the S_1 state. Meanwhile, the strengthening of the ground state hydrogen bonds drives the reverse proton transfer, so the keto form is not as stable in S_0 state as it is in S_1 state. In addition, the change of O_1–H_2 bond length in S_1 state of enol form is as follows:

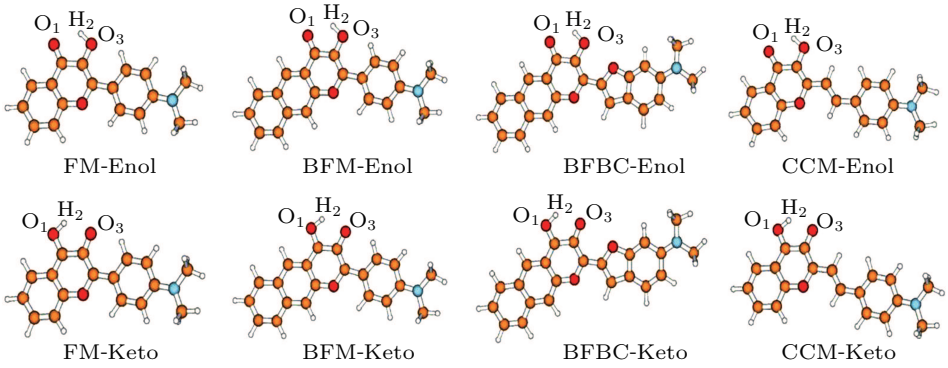


Fig. 2. Geometric structure of different substituents for 3-hydroxychromone (orange: C; red: O; white: H; blue: N).

FM (0.993 Å) > BFM (0.991 Å) > BFBC (0.985 Å) > CCM (0.981 Å). The longer the bond length of O_1–H_2, the weaker the hydrogen bond interaction. Therefore, it can be concluded that substituents change the hydrogen bond strength of 3HCs derivatives regularly and conform to the following rules: FM > BFM > BFBC > CCM.

Table 1. The optimized bond lengths (Å) and bond angles (°) of the four substituents for 3-hydroxychromone in S_0 and S_1 states.

		O_1–H_2	H_2–O_3	σ (O_1–H_2–O_3)
FM	Enol-S_0 Enol-S_1 Keto-S_1 Keto-S_0	0.981 0.993 1.948 1.822	1.993 1.794 0.979 0.993	119.6 126.1 119.9 124.4
BFM	Enol-S_0 Enol-S_1 Keto-S_1 Keto-S_0	0.974 0.991 1.942 1.817	1.963 1.808 0.980 0.995	120.1 125.1 119.8 124.7
BFBC	Enol-S_0 Enol-S_1 Keto-S_1 Keto-S_0	0.973 0.985 1.937 1.818	2.011 1.873 0.981 0.996	118.8 123.5 120.5 124.8
CCM	Enol-S_0 Enol-S_1 Keto-S_1 Keto-S_0	0.978 0.981 2.030 1.889	2.073 1.950 0.975 0.988	117.3 121.2 118.0 122.8

3.2. RDG analysis and frontier molecular orbitals

The intuitive way to determine the strength of hydrogen bonds is to compare the changes of isosurface. The RDG isosurfaces and scatter plots of FM, BFM, BFBC, and CCM obtained by utilizing the visual molecular dynamics (VMD) and

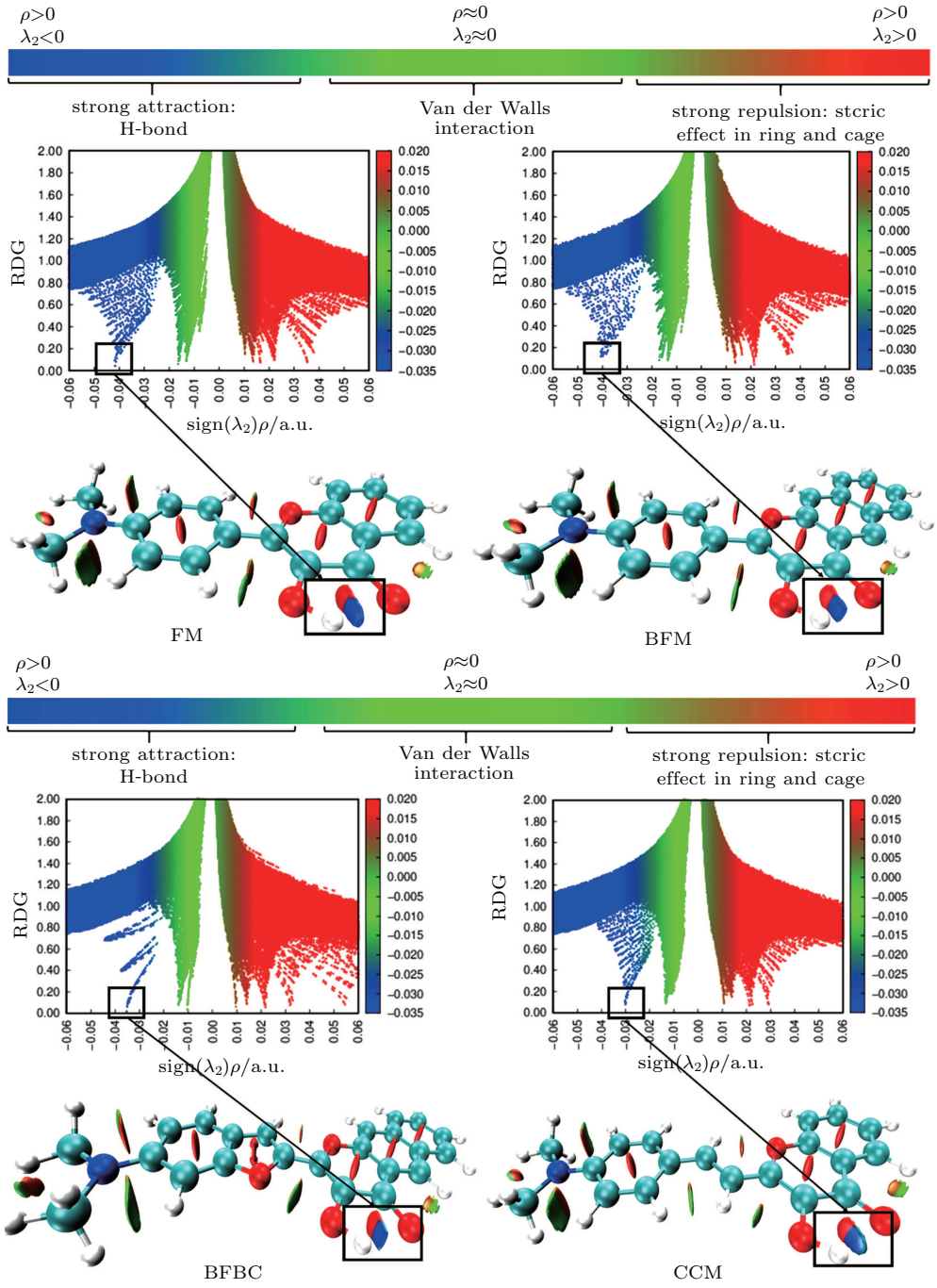


Fig. 3. RDG isosurfaces and scatter plots for (a) FM, (b) BFM, (c) BFBC, and (d) CCM.

Multiwfn softwares are plotted in Fig. 3. The hydrogen bond interaction, van der Waals interaction, and steric hindrance are represented by colors of blue, green, and red, respectively. It can be easily observed that the color of isosurface between the O_1 and H_2 atoms is blue, which means that there is a strong hydrogen bond interaction in the four kinds of molecules. However, the blue depth and the corresponding spike peaks are different among the four molecules, which indicates that different substituents have different effects on intramolecular hydrogen bonds. The more negative the spike peak values and the bluer the isosurface, the stronger the hydrogen bond interaction. It can be seen that although the spike peaks of FM and BFM are very close, the peak value of FM is slightly more negative than that of BFM. In addition, the spike peaks of BFBC and CCM are located at −0.035 a.u. and −0.030 a.u., which are significantly smaller than those of FM and BFM. According to the depth of the isosurface color and the negative of the spike peak values, it can be concluded that the order of hydrogen bond interactions from strong to weak is FM > BFM > BFBC > CCM.

The properties of electron excited states can be fully understood by detailed analysis of FMOs (the highest occupied molecular orbitals (HOMOs) and the lowest unoccupied molecular orbitals (LUMOs)). As shown in Fig. 4, the oscillator strengths of FM, BFM, BFB, and CCM in S_1 state are 0.861, 0.804, 0.905, and 1.28, and the corresponding orbital contributions are 98.91%, 99.48%, 99.17%, and 99.30%, respectively. Therefore, only the transition between HOMO and LUMO is involved in the S_1 state and their contribution is the largest. The HOMO orbitals show π feature, while the LUMO orbits show π^* feature, thus transitions from HOMOs to LUMOs show $\pi\pi^*$ feature. It is worth noting that after the transition from HOMO to LUMO, the electron distribution on the O_1 atom is reduced, and the electron distribution on the O_3 atom is increased. Thus, the O_1–$H_2\cdots O_3$ is indeed enhanced in the S_1 state. The natural bond orbital analysis is a reliable method for characterizing the charge transfer of hydrogen bonds in the S_1 state. The enhancement of hydrogen bond is also bound to increase the proton transfer tendency in the S_1 state.

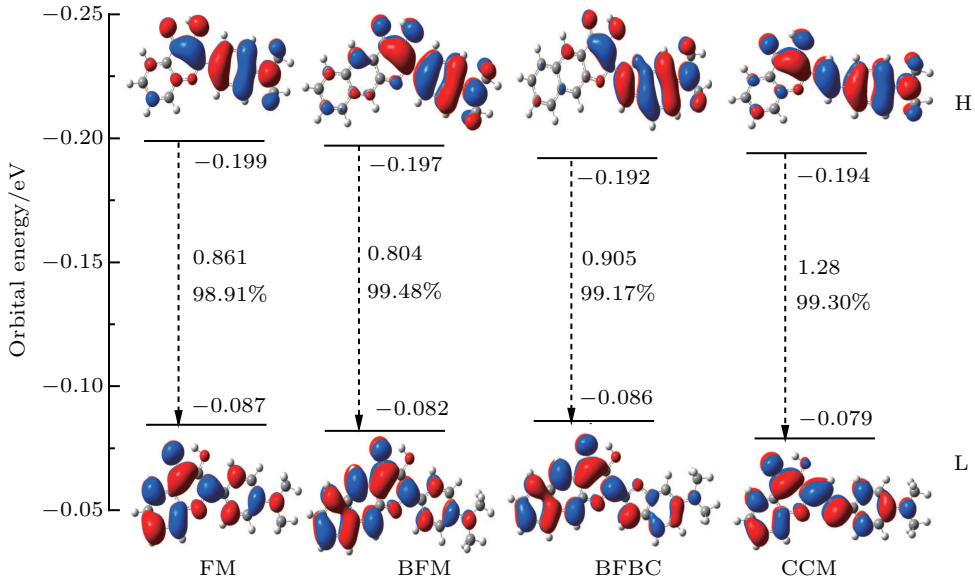


Fig. 4. FMOs of FM, BFM, BFBC, and CCM.

3.3. IR vibration and electronic spectra analysis

The electron spectra obtained by theoretical calculation cannot be directly compared with experimental values. To make the theoretically calculated data correspond to the actual spectral graph, we need to extend the data (oscillator strength, full width at half maximum (FWHM), and conversion energy) obtained from the calculation into a spectral band. The discrete spectra (IR spectra (Fig. 5) and electronic spectra (Fig. 6)) can be artificially expanded by Gaussian function

$$G(w) = \frac{1}{c\sqrt{2\pi}} e^{-\frac{(w-w_i)^2}{2c^2}}, \tag{3}$$

where

$$c = \frac{\text{FWHM}}{2\sqrt{2\ln 2}}, \tag{4}$$

and Lorentz function

$$L(w) = \frac{\text{FWHM}}{2\pi} \frac{1}{x^2 + 0.25 \times \text{FWHM}^2}. \tag{5}$$

Here, w stands for the spectrum abscissa, w_i represents the excitation energy corresponding to the electron excitation of interest, and i stands for the 1st to the nth electronic stimulus. The vibration frequency analysis not only ensures that the energy of the optimized S_0 and S_1 states is the real minimum, but also conduces to analyze the intramolecular hydro-

gen bond interaction. As depicted in Fig. 5, the vibration frequency of FM in S_0 state is 3618 cm^{-1}, while the vibration frequency decreases to 3296 cm^{-1} after FM transitions to the S_1 state. The vibration frequency decreases by 322 cm^{-1}, indicating that the hydrogen bond interaction of FM is enhanced in the S_1 state. Similarly, the stretching frequencies of BFM, BFBC, and CCM are reduced from the S_0 state (3625 cm^{-1}, 3656 cm^{-1}, and 3673 cm^{-1}) to the S_1 state (3325 cm^{-1}, 3436 cm^{-1}, and 3518 cm^{-1}). Therefore, the hydrogen bonds of the four derivatives are enhanced in the S_1 state. According to the size of the frequency in the S_1 state, the hydrogen bond strength and proton transfer ability of the four derivatives can be reduced in the order of FM > BFM > BFBC > CCM.

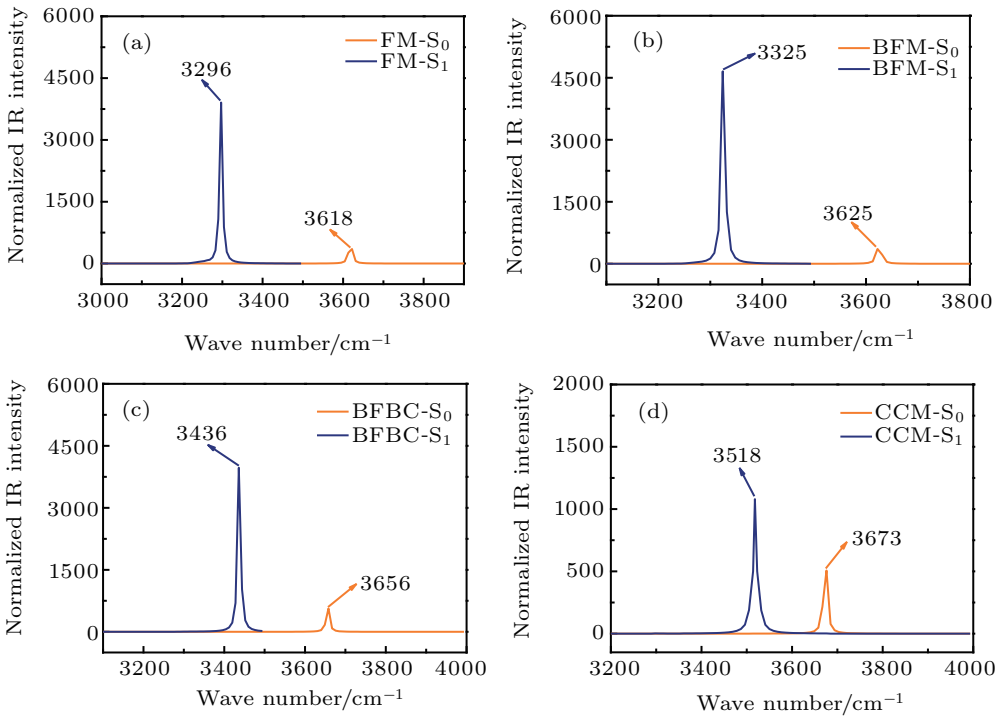


Fig. 5. IR spectra for the O–H bond of (a) FM, (b) BFM, (c) BFBC, and (d) CCM.

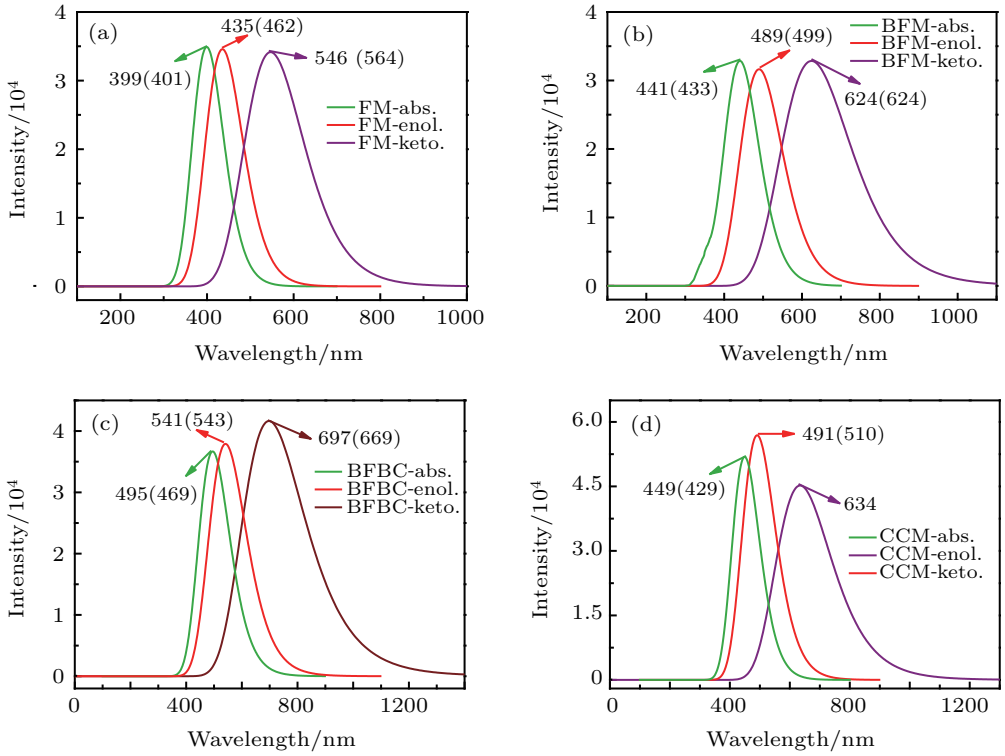


Fig. 6. Absorption and emission spectra of (a) FM, (b) BFM, (c) BFBC, and (d) CCM (the values in parentheses are experimental data).

The absorption and emission spectra of FM, BFM, BFBC, and CCM are plotted in Fig. 6. The absorption peaks of FM, BFM, BFBC, and CCM are 399 nm, 441 nm, 495 nm, and 449 nm (represented by the green line), respectively, which differ from the experimental data (401 nm, 433 nm, 469 nm, and 429 nm) by 2 nm, 8 nm, 26 nm, and 20 nm,[38] respectively. Thus, we can conclude that our calculation method is appropriate. In addition, we have also calculated the fluorescence spectra of FM, BFM, BFBC, and CCM before proton transfer, which are 435 nm, 489 nm, 541 nm, and 491 nm (represented by the red line). They are also consistent with the experimental data (462 nm, 499 nm, 543 nm, and 510 nm).[38] The fluorescence spectra (546 nm, 624 nm, and 697 nm) of FM, BFM, and BFBC also agree well with the experimental data (564 nm, 624 nm, and 669 nm).[38] However, the fluorescence spectrum of CCM is not given in the experimental literature.

3.4. Potential energy curves

The enhancement of excited hydrogen bonds lays the foundation for proton transfer, but it is only a qualitative description. To investigate the specific reaction path of protons, it is necessary to give quantitative data for comparison.[46–54] The PECs of FM, BFM, BFBC, and CCM in S_0 and S_1 states are given by scanning the O–H internuclear distance. The barrier between the S_0 and S_1 states of the four derivatives can be clearly observed from Fig. 7. It can be found that the barrier of all molecules in the S_1 state is significantly smaller than in the S_0 state, which shows that proton transfer is more likely to occur in the S_1 state. However, the barriers required for the reverse proton transfer of the four derivative molecules in the S_1 state are larger than the S_0 state, which indicates that the keto structure is more stable in the S_1 state. For the FM, BFM, BFBC, and CCM in the S_1 state, the barriers of proton transfer are 4.02 kcal/mol, 4.75 kcal/mol, 6.64 kcal/mol, and 6.70 kcal/mol, while the barriers of the reverse proton transfer are 7.72 kcal/mol, 7.33 kcal/mol, 5.92 kcal/mol, and 8.75 kcal/mol, respectively. It is well known that the smaller the barrier, the more likely the reaction will occur. The order of the barriers in which proton transfer occurs should be CCM > BFBC > BFM > FM. Therefore, the probability of proton transfer should follow this rule: FM > BFM > BFBC > CCM. In addition, the proton transfer process of the four derivatives should be a four-stage cycle, i.e., enol → enol*(S_1) → keto*(S_1) → keto → enol.

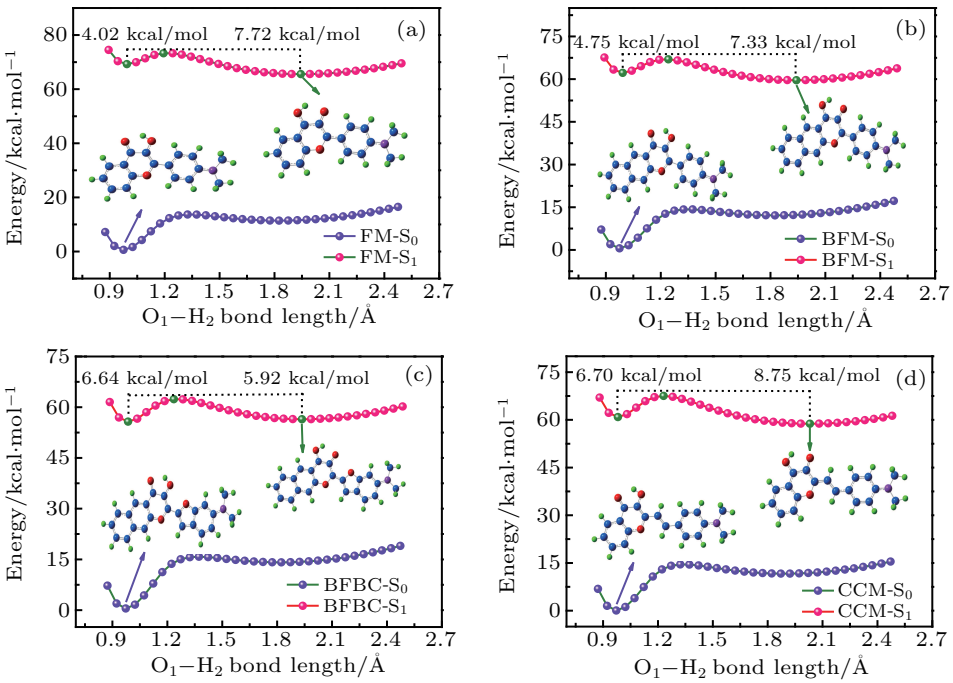


Fig. 7. The calculated PECs for (a) FM, (b) BFM, (c) BFBC, and (d) CCM.

4. Conclusions

The TDDFT/B3LYP-D3/6-311+G(d,p) methods have been used to explore the effect of different substituents on ESIPT. Analysis of geometrically optimized configurations, IR spectra, and the FMOs shows that hydrogen bonds of all molecules are enhanced in the S_1 state. The color change of isosurface in RDG diagram also intuitively confirms the strengthening mechanism of hydrogen bond. In addition, the calculated electron spectra are in good agreement with the experimental spectra. In order to quantitatively analyze proton transfer (PT), the PECs are constructed by scanning the O–H bond lengths of FM, BFM, BFBC, and CCM in S_0 and S_1

states. The PECs show clearly the path of proton transfer, and it is concluded that the ability of PT is FM > BFM > BFBC > CCM.

References

[1] Li D L, Yang Y G, Li C Z and Liu Y F 2017 *Environ. Res.* **154** 139
[2] Yang Y G, Li D L, Li C Z, Liu Y F and Jiang K J 2018 *J. Hazard. Mater.* **341** 93
[3] Tung C H, Wu L Z, Zhang L P and Chen B 2003 *Acc. Chem.* **36** 39
[4] Cramer C J and Truhlar D G 2008 *Acc. Chem. Res.* **41** 760
[5] Olsen S and Smith S C 2008 *J. Am. Chem. Soc.* **130** 8677
[6] Chu T S and Liu B T 2016 *Int. Rev. Phys. Chem.* **35** 187
[7] Li C Z, Ma C, Li D L and Liu Y F 2016 *J. Lumin.* **172** 29
[8] Weller A 1956 *Phys. Chem.* **60** 1144
[9] Zhao J F, Yao H B, Liu J Y and Hoffmann M R 2015 *J. Phys. Chem. A* **119** 681
[10] Liu S S, Zhao Y, Zhang C Z, Lin L L, Li Y Q and Song Y Z 2019 *Spectrochim. Acta, Part A* **219** 164
[11] Liu S, Ma Y Z, Yang Y F, Liu S S, Li Y Q and Song Y Z 2018 *Chin. Phys. B.* **27** 023103
[12] Yin H, Zhang Y M, Zhao H F, Yang G J, Shi Y, Zhang S X A and Ding D J 2018 *Dyes Pigm.* **159** 506
[13] Zhao J F, Dong H and Zheng Y J 2018 *J. Phys. Chem. A* **122** 1200
[14] Song Y Z, Liu S, Yang Y F, Wei D M, Pan J and Li Y Q 2019 *Spectrochim. Acta, Part A* **208** 309
[15] Liu S S, Pan J, Wei D M, Xu J H, Zhou Y and Song Y Z 2019 *Can. J. Phys.* **97** 721
[16] Tian M G, Sun J, Tang Y H, Dong B L and Lin W Y 2018 *Anal. Chem.* **90** 998
[17] Liu Y F, Ding J X, Shi D H and Sun J F 2008 *J. Phys. Chem. A.* **112** 6244
[18] Zhao G J and Han K L 2007 *J. Phys. Chem. A* **111** 2469
[19] Zhao G J and Han K L 2012 *Acc. Chem. Res.* **45** 404
[20] Zhao G J and Han K L 2008 *Chem. Phys. Chem.* **9** 1842
[21] Zhao G J and Han K L 2009 *J. Phys. Chem. A* **113** 4788
[22] Ma Y Z, Yang Y F, Shi W, Song Y Z and Li Y Q 2018 *Spectrochim. Acta, Part A* **202** 30
[23] Yang Y F, Ma Y Z, Zhao Y, Zhao Y L and Li Y Q 2018 *J. Phys. Chem. A* **122** 1011
[24] Dong H, Zhao J F, Yang H and Zheng Y J 2018 *Org. Chem. Front.* **5** 1241
[25] Hao J J and Yang Y 2018 *Org. Chem. Front.* **5** 2234
[26] Catalan J, Delvalle J C and Fabero F 1995 *Photochem. Photobiol.* **61** 118
[27] Chou P T, Martinez M L and Cooper W C 1994 *Appl. Spectrosc.* **48** 604
[28] Chou P T, Martinez M L and Studer S L 1991 *Appl. Spectrosc.* **45** 918
[29] Chou P T, Wei C Y, Wang C R C, Hung F T and Chang C P 1999 *J. Phys. Chem. A* **103** 1939
[30] Chen J S, Zhou P W and Yang S Q 2013 *Phys. Chem. Chem. Phys.* **15** 16183
[31] Kim T G, Kim Y and Jang D J 2001 *J. Phys. Chem. A* **105** 4328
[32] Huang J D, Teng W F, Chen D Y and Ma H P 2018 *J. Mol. Liq.* **249** 957
[33] Kanamori D, Okamura T A, Yamamoto H and Ueyama N 2005 *Angew. Chem. Int. Ed.* **44** 969
[34] Chen J S, Zhou P W, Zhao L and Chu T S 2014 *RSC Adv.* **4** 254
[35] Li A, Sun H X, Tan D Z, Fan W J, Wen S H, Qing X J, Li G X, Li S Y and Deng W Q 2011 *Energy Environ. Sci.* **4** 2062
[36] Li A, Lu R F, Wang Y, Wang X, Han K L and Deng W Q 2010 *Angew. Chem. Int. Ed.* **49** 3330
[37] Catalán J, Valle J C D, Fabero F and Garcia N A 1995 *Photochem. Photobiol.* **61** 118
[38] Kyriukha Y A, Kucherak O A, Yushchenko T I, Shvadchak V V and Yushchenko D A 2018 *Sens. Actuators, B* **265** 691
[39] Ma D G, Liang F S, Wang L X, Lee S T and Hung L S 2002 *Chem. Phys. Lett.* **358** 24
[40] FrischM J, Trucks G W, Schlegel H B, Scuseria G E, Robb M A, Cheeseman J R, Scalmani G, Barone V, Petersson G A and Nakatsuji H 2016 *Gaussian 16 Rev. A. 03*
[41] Becke A D 1993 *J. Chem. Phys.* **98** 5648
[42] Lee C, Yang W and Parr R G 1988 *Phys. Rev. B* **37** 785
[43] Gross E K U and Kohn W 1990 *Adv. Quantum. Chem.* **21** 255
[44] Marcus Y and Glikberg S 1985 *Pure Appl. Chem.* **57** 855
[45] Lu T and Chen F W 2012 *J. Comput. Chem.* **33** 580
[46] Johnson E R, Keinan S, Mori-Sánchez P, Contreras-García J, Cohen A J and Yang W 2010 *Chem. Soc.* **132** 6498
[47] Furche F and Ahlrichs R 2002 *J. Chem. Phys.* **117** 7433
[48] Kobayashi T, Yabushita A, Saito T, Ohtani H and Tsuda M 2007 *Photochem. Photobiol.* **83** 363
[49] Saga Y, Shibata Y and Tamiaki H 2010 *J. Photochem. Photobiol. C* **11** 15
[50] Song Y Z, Liu S, Ma Y Z, Yang Y F, Li Y Q and Xu J H 2018 *J. Mol. Struct.* **1173** 341
[51] Zhang H, Wang S F, Sun Q and Smith S C 2009 *Phys. Chem. Chem. Phys.* **11** 8422
[52] Sobolewski A L and Domcke W 1999 *Phys. Chem. Chem. Phys.* **1** 3065
[53] Li Y Q, Ma Y Z, Yang Y F, Shi W, Lan R F and Guo Q 2018 *Phys. Chem. Chem. Phys.* **20** 4208
[54] Lan R F, Yang Y F, Ma Y Z and Li Y Q 2017 *Spectrochim. Acta, Part A* **183** 37